A synthesis dataset of permafrost-affected soil thermal conditions for Alaska, USA

Kang Wang[1], Elchin Jafarov[2], Irina Overeem[1], Vladimir Romanovsky[3], Kevin Schaefer[4], Gary Clow[1], Frank Urban[5], William Cable[3,9], Mark Piper[1], Christopher Schwalm[6], Tingjun Zhang[7], Alexander Kholodov[3], Pamela Sousanes[8], Michael Loso[8], and Kenneth Hill[8]

[1]CSDMS, Institute of Arctic and Alpine Research, University of Colorado Boulder, Boulder, CO 80309, USA
[2]Los Alamos National Laboratory, Los Alamos, NM 87545, USA
[3]Geophysical Institute Permafrost Laboratory, University of Alaska, Fairbanks, AK 99775, USA
[4]National Snow and Ice Data Center, Cooperative Institute for Research in Environmental Sciences, University of Colorado Boulder, Boulder, CO 80309, USA
[5]U.S. Geological Survey, Lakewood, CO 80225, USA
[6]Woods Hole Research Center, Falmouth MA 02540, USA
[7]MOE Key Laboratory of Western China's Environmental Systems, College of Earth and Environmental Sciences, Lanzhou University, Lanzhou 730000, China
[8]National Park Service Arctic Central Alaska Inventory and Monitoring Networks Fairbanks, AK 99709
[9]Alfred Wegener Institute Helmholtz Center for Polar and Marine Research, 14473 Potsdam, Germany

Correspondence: Kang Wang (Kang.Wang@colorado.edu)

Abstract. Recent observations of near-surface soil temperatures over the circumpolar Arctic show accelerated warming of permafrost-affected soils. A comprehensive near-surface permafrost and active layer dataset is critical to better understand climate impacts and to constrain permafrost thermal conditions and spatial distribution in land system models. We compiled a soil temperatures dataset from 72 monitoring stations in Alaska using data collected by the U.S. Geological Survey, the National Park Service, and the University of Alaska-Fairbanks permafrost monitoring networks. The array of monitoring stations spans a large range of latitudes from 60.9°N to 71.3°N and elevations from near sea level to 1,327 m, comprising tundra and boreal forest regions. This dataset consists of monthly ground temperatures at depth up to 1 m, volumetric soil water content, snow depth, and air temperature during 1997 - 2016. These data have been quality controlled in collection and processing. Meanwhile, we implemented data harmonization validation for the processed dataset. The final product (PF-AK, v0.1) is available at the Arctic Data Center (https://doi.org/10.18739/A2KG55).

1 Introduction

Permafrost is frozen ground that remains at or below 0 °C for at least two consecutive years and may be found within about a quarter of the terrestrial land area in the Northern Hemisphere and 80% of the land area in Alaska (Brown et al., 1998; Zhang et al., 1999; Jorgenson et al., 2008). Continuous increase in near-surface air temperatures over the Alaskan Arctic (Romanovsky et al., 2015; Wang et al., 2017) causes warming and thawing of permafrost in Alaska, which is expected to continue throughout the 21st century with significant impacts on ecosystem and multi-billion-dollar loss in economy and infrastructure (Callaghan

et al., 2011; Hinzman et al., 2013; Liljedahl et al., 2016; Shiklomanov et al., 2017; Melvin et al., 2017). Permafrost thaw may have global consequences due to the potential for a significant positive climate feedback related to newly released carbon previously stored within the permafrost (Abbott et al., 2016; Schaefer et al., 2014; Knoblauch et al., 2018). Modeling studies indicate that greenhouse gas emissions following thaw would amplify current rates of atmospheric warming (McGuire et al., 2016). However, large uncertainties exist regarding the timing and magnitude of this permafrost-carbon feedback, in part due to challenges associated with representation of permafrost processes in the climate models and the lack of comprehensive permafrost datasets with which to test such models (Koven et al., 2015; McGuire et al., 2016), There is an immediate need for ready-to-use reliable near-surface permafrost datasets, including ground temperatures, soil moisture, and related climatic factors (such as air temperature and snow depth), which can serve as benchmarks for the modeling community and help to evaluate potential physical, societal, and economic impacts.

The permafrost extent map by Brown et al. (1998) is one of the most widely used metrics for comparing permafrost model results against ground-based data (Koven et al., 2015; McGuire et al., 2016). Another widely used dataset in model-data validation is the Russian Soil Temperature dataset of daily ground temperature measurements at different depths ranging from 0 to 3.2 m for 51 years (Sherstiukov, 2012). An additional ground temperature dataset includes daily-mean ground temperatures at various depths from 0 to 3.2 m at more than 800 stations in China, which for selected locations dates back to the 1950s (Wang et al., 2015). In addition to shallow borehole ground temperatures data (i.e. up to 3 meters) there are datasets that archive temperatures from the deeper (generally >5 m) boreholes (Clow, 2014; Biskaborn et al., 2015). Moreover, the Circumpolar Active Layer Monitoring (CALM) monitoring network measures active layer thickness (ALT) - the maximum soil depth above permafrost that thaws every summer and refreezes in the winter (Brown et al., 2000; Shiklomanov et al., 2008). Here, we consolidated data from shallow borehole ground monitoring stations across Alaska from multiple government agencies. The importance of the shallow borehole data is that it records the more immediate response to the changing environmental conditions, whereas deep ground temperatures take extensive time to respond.

A typical permafrost monitoring station consists of an air temperature sensor, a snow depth sensor, soil moisture sensors, and soil temperature sensors. In-situ observations of ground temperatures from the Alaskan Arctic region have been dispersed over different monitoring efforts, which are spread over varying timespans, and have non-uniform depths. The maximum depth of a typical monitoring station ranges from 1 to 3 m below the ground surface. However, not all stations use this design. For example, the National Park Service of Alaska network does not collect soil moisture data. Also, data from permafrost monitoring stations in Alaska are not archived in a common standardized format and are hosted by different academic and government agencies, such as the Arctic Data Center, the Global Terrestrial Network for Permafrost (GTN-P), the Long Term Ecological Research Network (LTER), and the U.S. Geological Survey (USGS). Thus, we compiled a ready-to-use permafrost dataset in order to allow for efficient data retrieval and processing for permafrost-related analysis.

We compiled a first integrated shallow ground temperatures dataset for permafrost-affected soils across Alaska from the three most reliable sources monitoring networks over past several decades: the Geophysical Institute Permafrost Laboratory at the University of Alaska Fairbanks (GI-UAF), National Park Services in Alaska (NPS), and the USGS. This synthesis permafrost dataset for Alaska (PF-AK, version 0.1) includes measured air and ground temperatures to 1.0 m, snow depth

and soil volumetric water content for 72 permafrost monitoring stations across the state of Alaska. Detailed information and meta-data are provided for the compiled dataset so that potential users can have a full understanding of the data and its associated limitations. Furthermore, two types of data validation were implemented: (i) testing for inconsistencies between air and ground temperature trends; and (ii) use of the snow heat transfer metric to validate the relations between seasonal temperature amplitudes and snow depth. These technical validation would be useful for proving data harmonization and reusing these data.

2 Data sources and processing

2.1 Permafrost monitoring networks

Our synthesis permafrost dataset for Alaska (Fig.1) is based on observed in-situ data collected by the USGS, NPS, and GI-UAF teams. In the late 1990s, researchers at the GI-UAF established a near-surface permafrost monitoring system consisting of 27 stations across Alaska, primarily along the Trans-Alaskan highway (Fig.1)(Romanovsky et al., 2015). Similarly, the USGS installed permafrost stations to monitor permafrost conditions within the two federally managed areas on the North Slope, the National Petroleum Reserve-Alaska and the Arctic National Wildlife Refuge. Since August 1998, the USGS has maintained 17 automated stations in the area spanning latitudes from 68.5°N to 70.5°N and longitudes from 142.5°W to 161°W (Fig.1) (Urban and Clow, 2017). NPS has monitored ground temperatures since 2004 (Hill and Sousanes, 2015). All monitoring stations are installed on undisturbed land (Fig.2) at a minimum specified distance from nearby infrastructure. This protocol for installation ensures no biases associated with anthropogenic or ecosystem disturbances, which is one of the main differences with traditional meteorological stations which are often associated with airstrips and villages in Alaska. The brief description of site environments, including dominant soil type and vegetation description, was summarized in Tab.2. Due to the different field work design of various teams, the soil and vegetation description may not fully comparable and not available at all sites.

These networks utilize radiation-shielded thermistors (Campbell Scientific CSI 107 temperature probes) to monitor air temperature. In the GI-UAF and NPS network, the air temperature sensors were installed at 1.5 or 2.0 m above the ground surface, whereas the USGS network monitors air temperature at 3.0 m above the ground surface in order to minimize damage by wildlife.

Instrument of ground temperatures monitoring was summarized in Tab.3. To monitor near-surface ground temperatures, the networks use either a probe with several thermistors embedded into a single rod, typically 1.0 to 1.5 m long, or several individual Campbell Scientific 107 thermistors anchored at specified depths within a single hole. The thermistor temperature sensors are designed to record temperatures ranging from -30 to 75 °C; the 107 sensors record temperatures from -35 to 50 °C. An ice-bath calibration is a required procedure before installation of these probes. The ice-bath calibration includes placing the sensors into an insulated container filled with a mixture of ice shavings and distilled water, measuring the temperature, and recording the offset from 0 °C. This measured offset is then used to correct the temperature measurements. The average accuracy of these sensors is $\pm$0.01 °C (Romanovsky et al., 2008). For the USGS network, the thermistor sensors are installed inside a tight-fitting fluid-filled 125-cm-long plastic tube to measure ground temperatures at 5, 10, 15, 20, 25, 30, 45, 70,

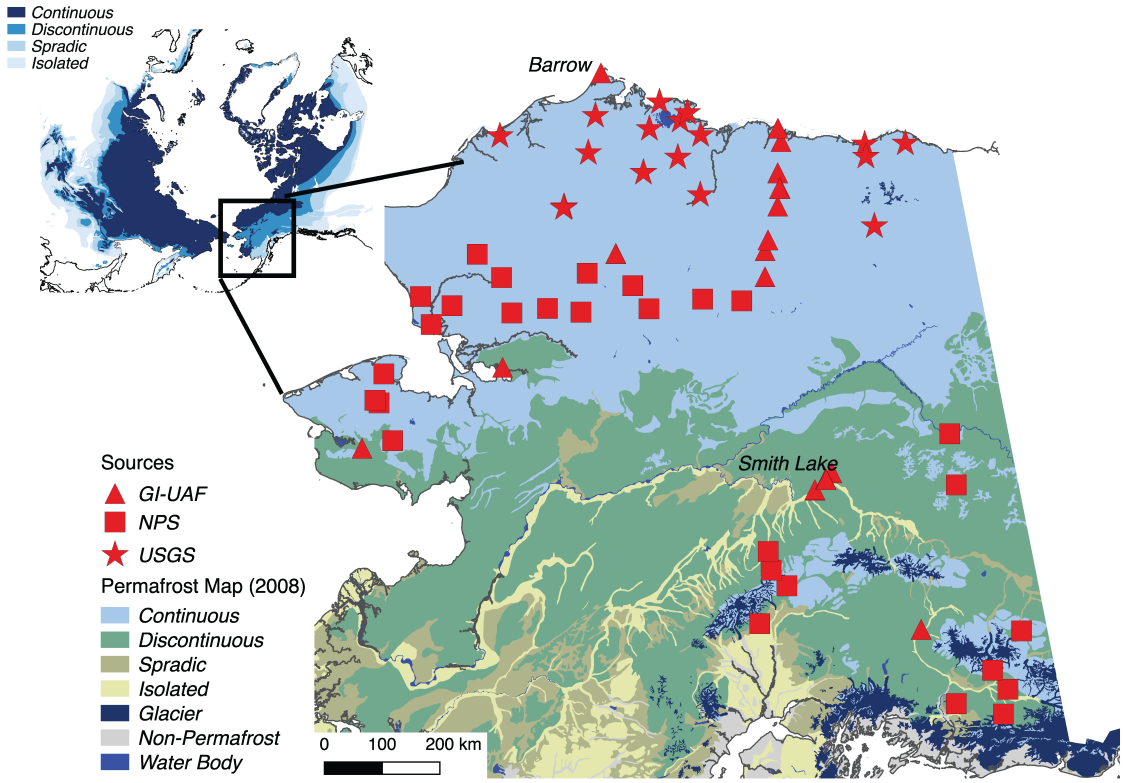

Figure 1. Locations of Geophysical Institute-University of Alaska Fairbanks (GI-UAF), U. S. Geological Survey (USGS), and National Park Services (NPS) permafrost monitoring stations in Alaska. The basemap is a new permafrost distribution of Alaska compiled by Jorgenson et al. (2008).

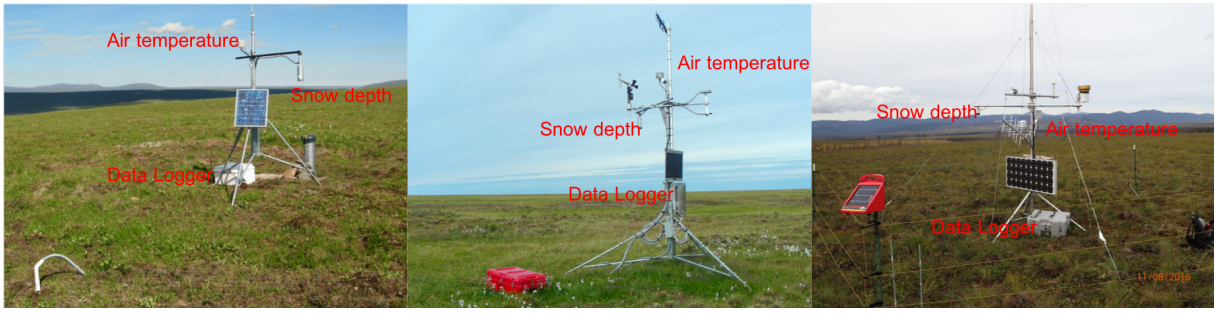

Figure 2. Typical permafrost observing stations. Left is Imnaviat 1 site (68.64 °N, 149.35°W) in the GI UAF network (source: http://permafrost.gi.alaska.edu/site/im1); middle is the Drew Point station (70.86°N, 153.91°W) in the USGS network (source:http://pubs.usgs.gov/ds/0977/DrewPoint/DrewPoint.html); right is the Wigand site (63.81°N, 150.109°W) in the NPS network.

95, and 120-cm depth (Urban and Clow, 2017). The NPS has three to four soil temperature sensors (CSI-107) installed in individual holes at 10, 20 and 50 cm depths, and at several locations an additional sensor at 100 cm. The ground-measurement depths vary station by station within the GI-UAF network, typically ranging from the ground surface (i.e., 0 m) to 1 m below the ground surface. It is important to note that most of the installed probes frost heave with time, and heaving depths are adjusted accordingly by subtracting the heaving values yearly. The released data account for the heave and have corrected ground temperatures. The USGS and NPS teams estimate frost heave by using ground temperature data from the topmost thermistor (at 5 or 10 cm depth). If temperature of the top thermistor during thaw-period exceeds air temperature then the sensor is considered exposed or partly exposed to solar radiation. The GI-UAF team measures frost heave at every site and then subtract heave depth from known sensors depth to correct for heaving (Romanovsky et al., 2008). Each team corrects for heaving every summer, and corrections are applied before releasing data.

Both the USGS and the GI-UAF networks measure liquid soil moisture using a HydraProbe sensor developed by Stevens Water Monitoring Systems Inc. The Stevens HydraProbe has a reported accuracy of $\pm 0.03\ m^3/m^3$ (Bellingham, 2015). Each volumetric water content sensor was calibrated in accordance with the soil texture in laboratory while uncertainties associated with the sensor's sensitivity still exist under specific conditions, e.g., for peat. The measured liquid soil moisture from a HydraProbe cannot be directly compared with the total soil moisture content values produced by land system models because in most of the models, soil moisture includes both ice and liquid water, where HydraProbe measures only liquid soil moisture. The USGS network measures soil moisture at one depth, approximately 0.15 m below the ground surface in all cases. The soil moisture sensors depths vary between stations for the GI-UAF network because they are installed at depths depending on the soil profile and texture within the active layer. The GI-UAF network measures soil moisture typically at three different depths within the active layer, ranging from 0.10 to 0.60 m. The NPS network does not include moisture probes at any of their monitoring stations. Our processed dataset presents only the upper layer (up to 0.25 m) soil water content.

Snow depth is measured once per hour with a SR50 or SR50A ultrasonic distance sensor (Campbell Sci. Inc.) at all of the stations. This downward-looking sensor is mounted on a cross-arm typically at 2.5 m above the ground surface for the USGS and NPS networks, and 1.5 m above the ground surface for the GI-UAF network respectively. The factory evaluated accuracy is ± 0.01 m or 0.4% of the distance to the ground surface. It is important to note that vegetation at the ground surface might influence shallow snow depth measurements.

2.2 Data processing workflow

All three networks apply data processing and quality-control checks before release. Typically, quality control occurs shortly after annual summer field campaigns; the fully-processed and quality-controlled data become publicly available a year after the data collection. In the present version of the permafrost dataset, we use USGS Data Series 1021, which includes data through July 2015 (URL: https://pubs.er.usgs.gov/publication/ds1021). The GI-UAF and NPS data were collected and processed by December, 20, 2017, and latest calibrated data was August, 2016. The GI-UAF data are available on http://permafrost.gi.alaska.edu/sites_map. NPS data is available from https://irma.nps.gov/DataStore/Reference/Profile/2240059 and https://irma.nps.gov/DataStore/Reference/Profile/2239061.

Fig.3 shows a schematic representation of the data processing workflow used to compile the dataset. To standardize the ground temperature depths in the dataset, we linearly interpolate ground temperatures for target depths: 0.25, 0.50, 0.75, and 1.00 m; however, we did not extrapolate beyond the maximum observed depth at any site. We implemented any interpolation requiring measurements for at least four depths, which assures a relatively small interval around the target depths. In addition, soil temperatures were not extrapolated. In other words, ground surface temperature is only calculated when supporting measurements are indeed available. Then, the calculated soil temperature at a specific depth depends on linear slope between just the observations at adjacent depths. Therefore, using a linear interpolation method does not result in a linear prediction from ground surface to 1 m, even if that probably is rather reliable fit. Furthermore, we examined the uncertainty resulting from our linear interpolation method for the most data sparse case, i.e. when we only have observations at four depths. To do so we selected the entire year of data without any missing values and depths and used linear interpolation to predict temperatures at five depths. Then we randomly selected only four depths, and interpolated again by using these four depths. While missing depths would reduce the number of available interpolation results, the influence from missing depths is limited.

The USGS and NPS network releases data at hourly resolution, whereas the GI-UAF network releases data at daily resolution. Since the most common model data output intervals of the land system and global climate models are monthly, the monthly means were calculated for all variables, including air and ground temperatures, snow depth, and soil water content. In addition to monthly data, annual means were calculated to allow evaluation of the relationship between air and ground temperatures. Thus, the dataset also provides annual statistics, including mean-annual air temperature (MAAT); mean-annual ground surface temperature (MAGST); mean-annual ground temperature to 1 m (MAGT at 0.25, 0.50, 0.75, and 1.00 m); mean and maximum seasonal snow depth (SND); and maximum, mean, and minimum soil volumetric water content (VWC).

Data from many sites have gaps and discontinuities due to harsh environmental conditions and wildlife that may interrupt the monitoring. There are various methods for calculating monthly means from incomplete time series data. For example, the USGS standards allow only 5% of missing values for both monthly and annual mean temperature data (Urban and Clow, 2017). The World Meteorological Organization (WMO) does not allow gaps of more than three consecutive days or more than 5 days total from each monthly data series (Plummer et al., 2003). Other researchers are more tolerant of missing data, acknowledging the difficulty of data collection in remote cold regions. Menne et al. (2009) allows up to 10 missing days in a monthly time series. Bieniek et al. (2014) calculated monthly averages using at least 15 days. Here we calculated monthly means for any station which has at least 20 days of measurements for that specific month. The annual means were calculated from daily data. Due to the scarcity of the data, we calculate the annual means only for those years with a coverage of at least 90% of the daily data. For this reason, we present annual means for air and ground temperatures as well as soil moisture, derived from daily data.

During the dataset compilation, we identified similarly named sites with different installation times and locations that do not match precisely. It is important to note that these sites, even when located nearby each other, may have considerably different environmental conditions, and thus, different ground temperature thermodynamics. A unique name is assigned to each site. Deadhorse site maintained by GI-UAF, and Awuna site maintained by USGS have new monitoring stations, and the old ones have been decommissioned. The new and retired systems were simultaneously running for few months in order to evaluate the

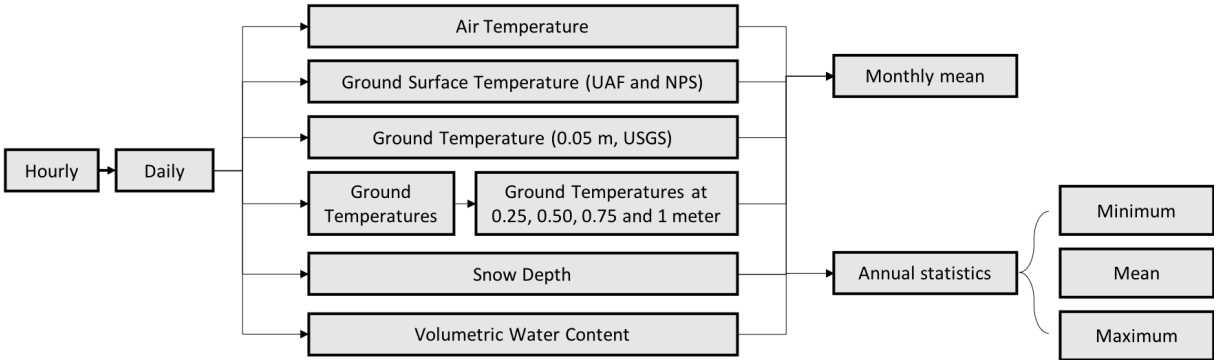

Figure 3. Schematic representation of the data processing workflow used to compile the permafrost dataset in the Alaska.

data consistency. The environmental conditions for the newer Deadhorse station remained the same assuring data consistency. The environmental conditions between two monitoring stations at Awuna are quite different: the original Awuna site was located on a ridge, whereas the new site is in a valley 1.9 km away. Nevertheless, the temperature data are consistent between the old and new station at Awuna. The old site (Awuna1) did not monitor soil moisture, which would be expected to be more site-specific and spatially variable. Thus, in this dataset, we present both the new and old sites' records.

In addition, three derived variables, freezing index (DDF), thawing index (DDT), and frost number (FN), were derived from monthly temperature curve. Nelson and Outcalt (1987) and Zhang et al. (1996) have demonstrated from datasets with daily time resolution that results using monthly data correspond closely to results from daily data analysis. The Frost Number index was also calculated (Eq.1-3) for air temperature and ground temperatures following Nelson and Outcalt (1987).

$$FrostNumber = \frac{\sqrt{DDF}}{\sqrt{DDF} + \sqrt{DDT}} \tag{1}$$

DDT and DDF are given by

$$DDT = \int T(t)dt, T(t) > 0°C \tag{2}$$

and

$$DDF = \int |T(t)|dt, T(t) \leq 0°C \tag{3}$$

The Frost Number serves as a simplified index for the likelihood of permafrost occurrence. A Frost Number index of 0.5 implies equal freezing and thawing index. When the Frost Number index is > 0.5, it indicates the annual period of freezing is dominates thaw, implying climate condition that promote permafrost.

2.3 Data validation

Despite the fact that individual station observations had originally been quality-controlled, we still need to examine our own results of the data harmonization. Here we implemented two ways of validation, the first way compares the trends in air and ground temperatures; and the second method examines the effects of snow on ground thermal state.

The primary objective of the trend analysis was to evaluate the consistency between trends at each station (for different depths) and between stations rather than inform inter-annual variability. Most of the estimated trends have a short observational period (see Tab.1). We chose to show trends only for those stations with more than ten available annual means. Currently, some of the time series are too short to provide significant trends. As more data becomes available in the future, a more rigorous analysis will be possible. It is well known that climatic trend analysis requires more than 30 years of time series (IPCC, 2013). On the other hand, Box et al. (2005) showed that 15 years are sufficient for inter-annual variability diagnosis to be statistically significant. Since the time series for most of the stations do not exceed 15 years we calculate trends for temperatures at different depths to determine inconsistencies between air and ground temperature trends in terms of sign's differences.

The second aspect is to examine the physical mechanism among air temperature, snow cover and ground thermal states, which is an auxiliary validation of the dataset. Seasonal snow cover will keep the ground warm by reducing cooling (or heat loss) during the winter (Yershov and Williams, 2004). Considering a semi-infinite column, the damping of the ground temperature annual cycle is depending on snow depth and soil thermal properties. In this study, the snow period was defined as October through March. We averaged the snow depth measurements over the period from October through March to obtain the effective snow depth (SND_{eff}) (Slater et al., 2017). The amplitudes of air temperature (Amp_{air}) and ground surface temperature (Amp_{gnd}) were calculated following Slater et al. (2017), for those stations with available snow depth data. The snow and heat transfer metric (SHTM) captures the correlation between the normalized temperature amplitude difference (ΔAmp_{norm}) (i.e., Eq.4-6) and SND_{eff}. As a physical mechanism examination, SHTM and ΔAmp_{norm} were only referring to ground surface temperature, because damping effect with depth (i.e., the difference between air temperature and ground temperature at deeper soil) is more dependent on ground thermal properties.

$$\Delta Amp_{norm} = \frac{Amp_{air} - Amp_{gnd}}{Amp_{air}} \tag{4}$$

Amp_{air} and Amp_{gnd} are given by

$$Amp_{air} = [Max(T_{air}) - Min(T_{air})]/2 \tag{5}$$

and

$$Amp_{gnd} = [Max(T_{gnd}) - Min(T_{gnd})]/2 \tag{6}$$

3 Results

3.1 Overview of this dataset

Tab.4 presents an overview of the data compiled in the dataset for Alaska. Our dataset comprises 41,667 data points in total. There is significant missing data, e.g. some stations do not have soil moisture sensors installed, and there are different observational periods for each sensor (e.g., air temperature data was installed often earlier than other variables, sensor failure). Excluding the missing time-series when certain instruments not installed, the percentage of complete data is about 77%.

Fig.4 shows annual summary of our core variables, including mean annual air temperature, ground surface temperature, and ground temperatures at 0.25, 0.50, 0.75, and 1.00 m. Overall, mean annual air temperature is less than -10 °C in the Alaskan Arctic while close to freezing point (-0.5 °C at RUGA2 site) in the southern mountain tundra regions. Mean annual ground surface temperature for 46 available sites ranges from -7.6 °C through 2.5 °C, which is higher than air temperature. Many sites comprise measurements of ground temperature at 0.25 and 0.50 m, 69 and 67 sites respectively. The range of ground temperature at 0.25 m and 0.50 m are roughly from -7.8 to 3.3 °C (Generally, deeper soil is colder than surface while the range is not exactly represented because the available sites varied for depths). Mean annual ground temperature at 0.75 m varies from -7.5 to 1.2 °C over 49 available sites. Our data comprises only 32 sites with ground temperature at 1 m, preferably located in the southern region of the Alaskan Arctic ($\sim$62°N), and the range of mean annual ground temperature at 1 m is -7.8 to 1.2 °C.

The VWC shown in Tab.4 is from the upper part of the soil (i.e., up to 25 cm depth). The VWC measurements are mainly available on the North Slope of Alaska. Maximum VWC is more important for understanding active layer dynamics, especially during summer. Notably, the maximum VWC has a three times larger spatial variance than the annual means. Three sites, Chandalar Shelf, Pilgrim Hot Springs, and Red Sheep Creek, were much wetter than other sites (maximum VWCs exceeding 0.7 m^3/m^3). This is mainly because these sites are close to a water body.

Snow depth is spatially variable over Alaska, although with a general trend of increasing snow depth in the southern part of the state, according to the synthesis dataset (Fig.5). In the Alaskan Arctic, snow cover is shallower than in the southeast region. The maximum seasonal snow depth was $>$ 1.5 m at the Gates Glacier station (which is located near the glacier) in Wrangell-St. Elias National Park. The lowest maximum snow depth occurs at WestDock near the Beaufort Sea in Prudhoe Bay at only 0.09 m in 2010 (note that, there were available snow depth measurements only for 2010, i.e., we did not have enough data for any other years). The other two sites, Asik in Noatak National Park and Serpentine in Bering Land Bridge National Preserve, also showed a shallow snow cover in recent years. The thin snow cover is probably due to wind exposure.

3.2 Data validation

In this dataset, we derived the frost number index for air and ground temperatures at various depths (Fig.6 and Tab.5). Because many stations do not have sensors at depth > 1 m, we report the freezing/thawing indices of air, ground surface, and 0.5 m below the ground surface in Fig.6, with all available results listed in Tab.5. Overall, almost all stations have air frost number above 0.5. Stations on the North Slope have both air and ground surface frost numbers exceeding 0.6. In interior and southern Alaska, air frost numbers were above 0.5, although the ground surface frost numbers were much lower due to the thicker snow

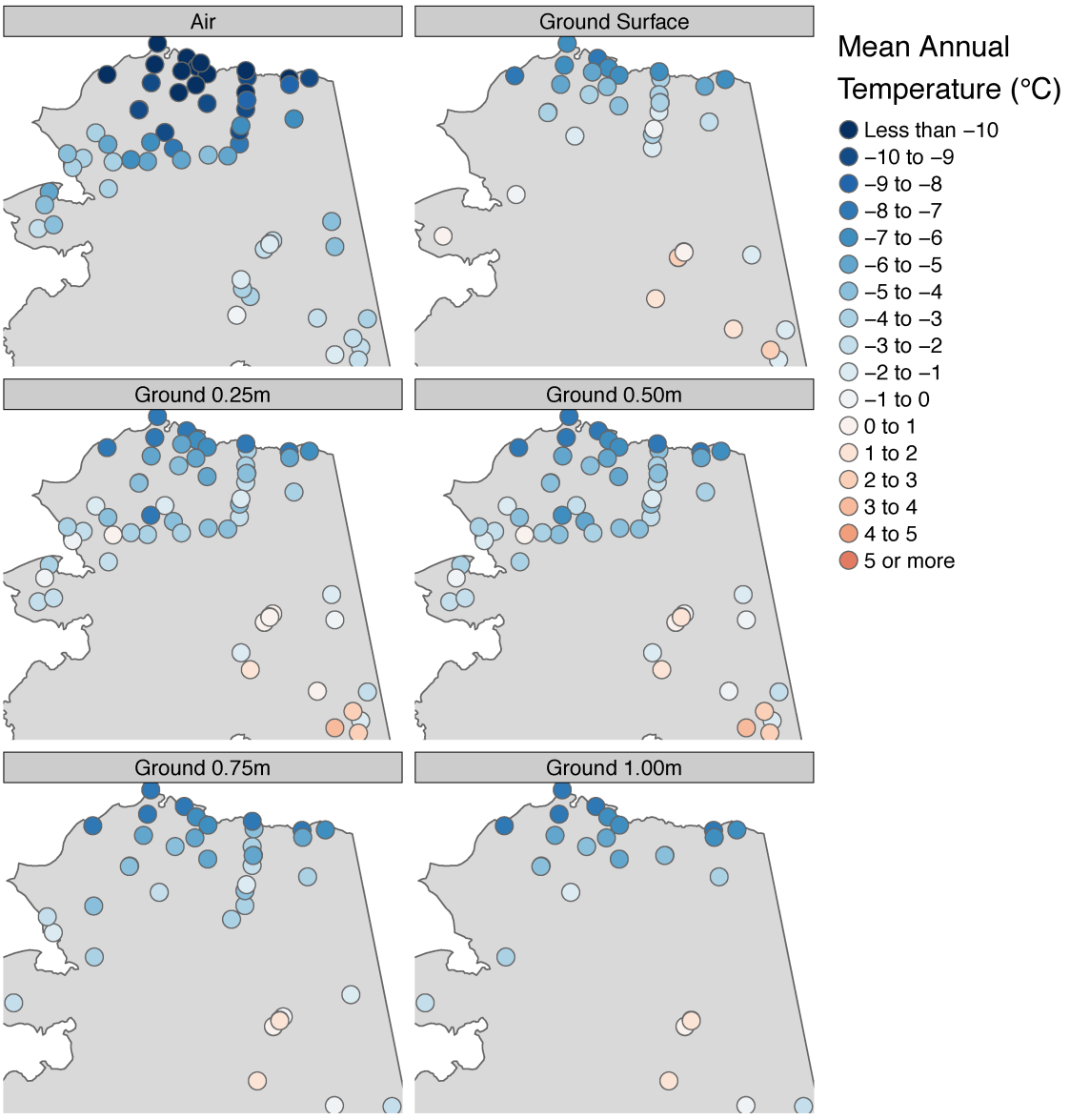

Figure 4. Overview of spatial distribution of mean annual air temperature, ground surface temperature, and ground temperatures at 0.25 m, 0.50 m, 0.75 m, and 1.00 m.

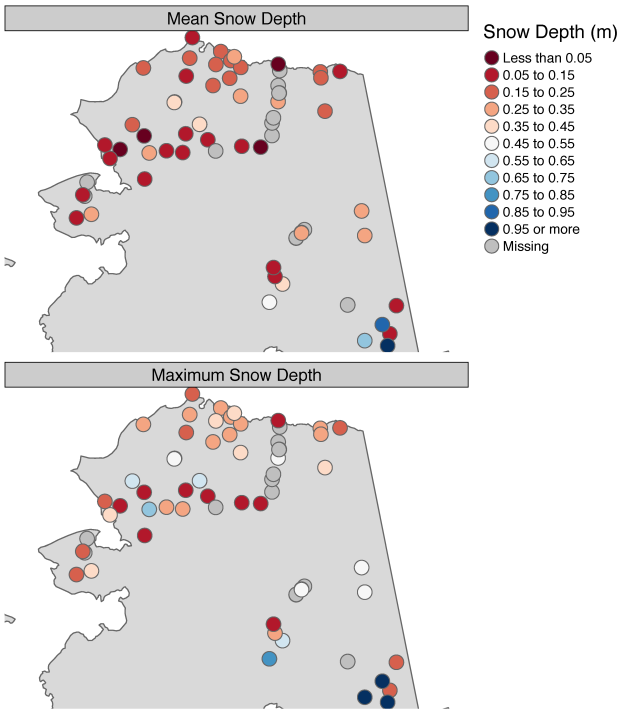

Figure 5. Overview of spatial distribution of snow depth, including annual mean snow depth and maximum snow depth.

cover in this region. In the Alaskan Arctic, thawing indices at ground surface were generally lower than air according to the station observations. There were 13 stations with a zero thawing index of ground temperature at 0.5 m. These results indicate a shallow active layer (< 0.5 m) at these sites, which is consistent with the Active Layer Monitoring Network CALM data. Another five stations have a thawing index of ground temperature at 0.5 m less than 10 °C–days. The calculated frost number indices are consistent with the existing permafrost distribution map over the Alaska (Jorgenson et al., 2008).

We examined the consistency among the trends of MAAT, MAGST, and MAGT at 1 m depth. Typically, if MAAT has a long-term positive trend then MAGST is expected to have a positive trend, even if the rate is dampened (Romanovsky et al., 2015). Similarly, signs of trends in MAGST and MAGT at 1 m depth, and MAAT and MAGT at 1 m depth are hypothesized to be consistent (Romanovsky et al., 2015). Here we show the annual mean temperatures at four stations, Drew Point, Fish Creek, Niguanak, and Tunalik, with ten or more years of data (Fig.7). Mean annual air, ground surface, and ground temperature at 1 m indicates consistent warming at rates of 0.07 – 0.18, 0.14 – 0.23, and 0.12-0.22 °C/year, respectively. An obvious feature was that at Fish Creek, ground surface temperature and ground temperature at 1 m showed amplified warming rates compared to the magnitude of the air temperature increases, which can be explained by the significant increase of seasonal snow depth during the same period. There are six stations with relatively long records ($\geq$10 years) of air, ground surface, and ground temperature at 0.5 m for the same period. In other words, at these sites, the data used to estimate linear trends of air, ground surface, and

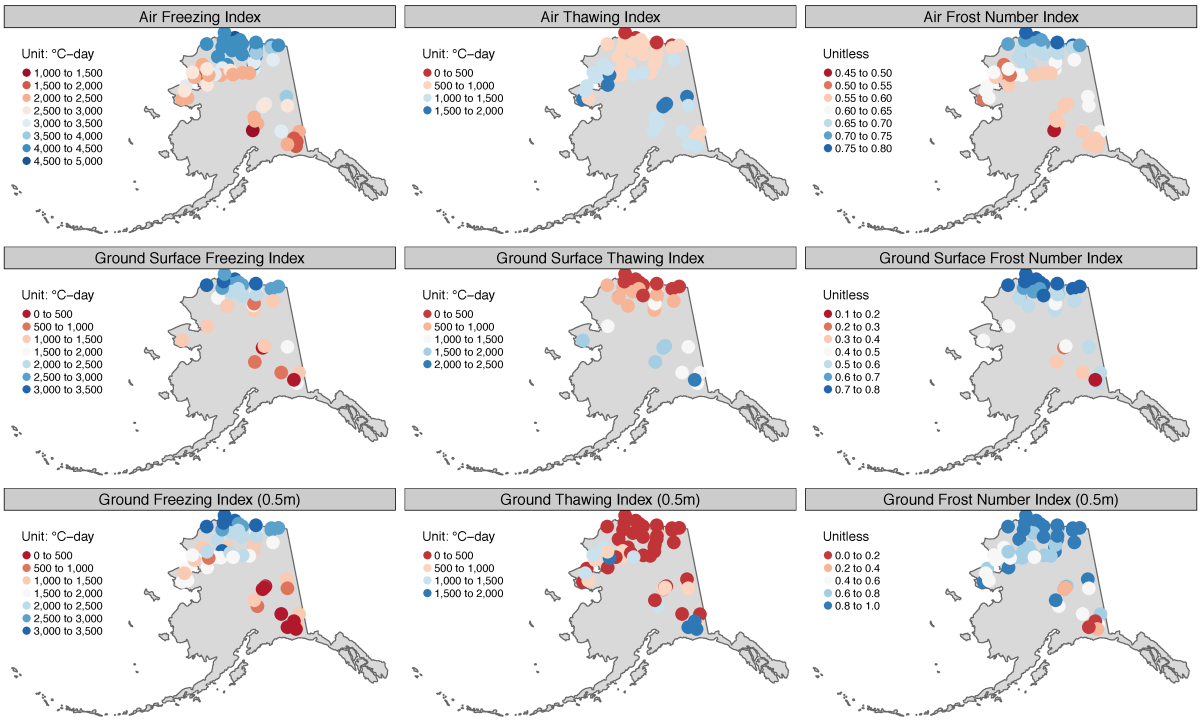

Figure 6. Overview of spatial distribution of freezing/thawing index from air, ground surface temperature, and ground temperature at 0.50 m. Frost Number (FN) was derived from the freezing/thawing index according to Nelson and Outcalt (1987).

ground temperature at 0.5 m were exactly same years. Fig.8 shows that air temperature, ground surface, and ground temperature at 0.5 m have consistently positive trends. Furthermore, the trends in ground surface and 0.5 m were generally close.

Besides, there are several sites in a small area that indicated inconsistency in air temperature trends. This was mainly because of different observational periods and relatively short duration of records. Typically, there are several Smith Lake (SL) permafrost monitoring stations which are located north of the UAF campus and west of Smith Lake with varying environmental conditions (SL1 is in a White Spruce forest with high canopy; SL2 is in a dense diminutive Black Spruce forest; and SL3 is located at the edge of the forest surrounded by Black Spruce trees and tussock-shrubs; and SL4 is characterized by hummocks of sedges (tussocks) and shrubby vegetation with sparse Black Spruce.). The environmental conditions at SL3 site provide favorable conditions for permafrost existence. The SL3 site has the longest air temperature record indicating a cooling trend over the observational period (Fig.9A). After calculating the differences between measured data for all three sites we applied corresponding corrections and extend the data at all three sites. The overlap period (2006-2012) showed a consistent variation with the roughly constant offset between SL2 and SL3. By using the offset, we extended the records at Smith Lake 3 to 2015. Fig.9B shows that extending the time series reduces the trend magnitude and changes the negative sign in SL3 trend to positive, indicating the important difference between a complete versus a sparse time series.

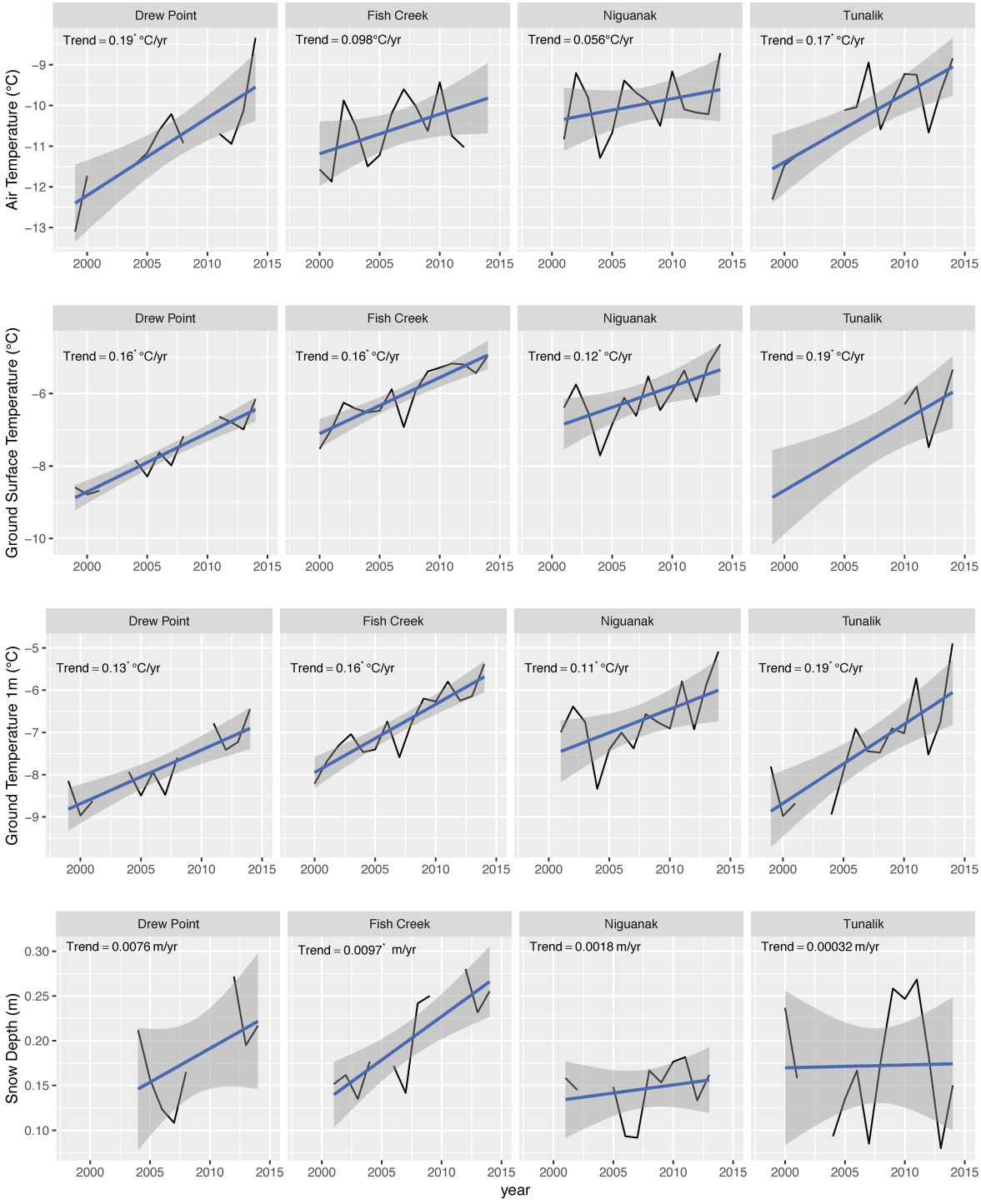

Figure 7. Examples of time-series in mean annual air, ground surface, ground temperature at 1 m below ground surface, and snow depth. Black line indicates data time-series. Blue line is estimated linear trend. The shadow is showing standard error of the linear regression estimates. The asterisk means the trend with p value < 0.05.

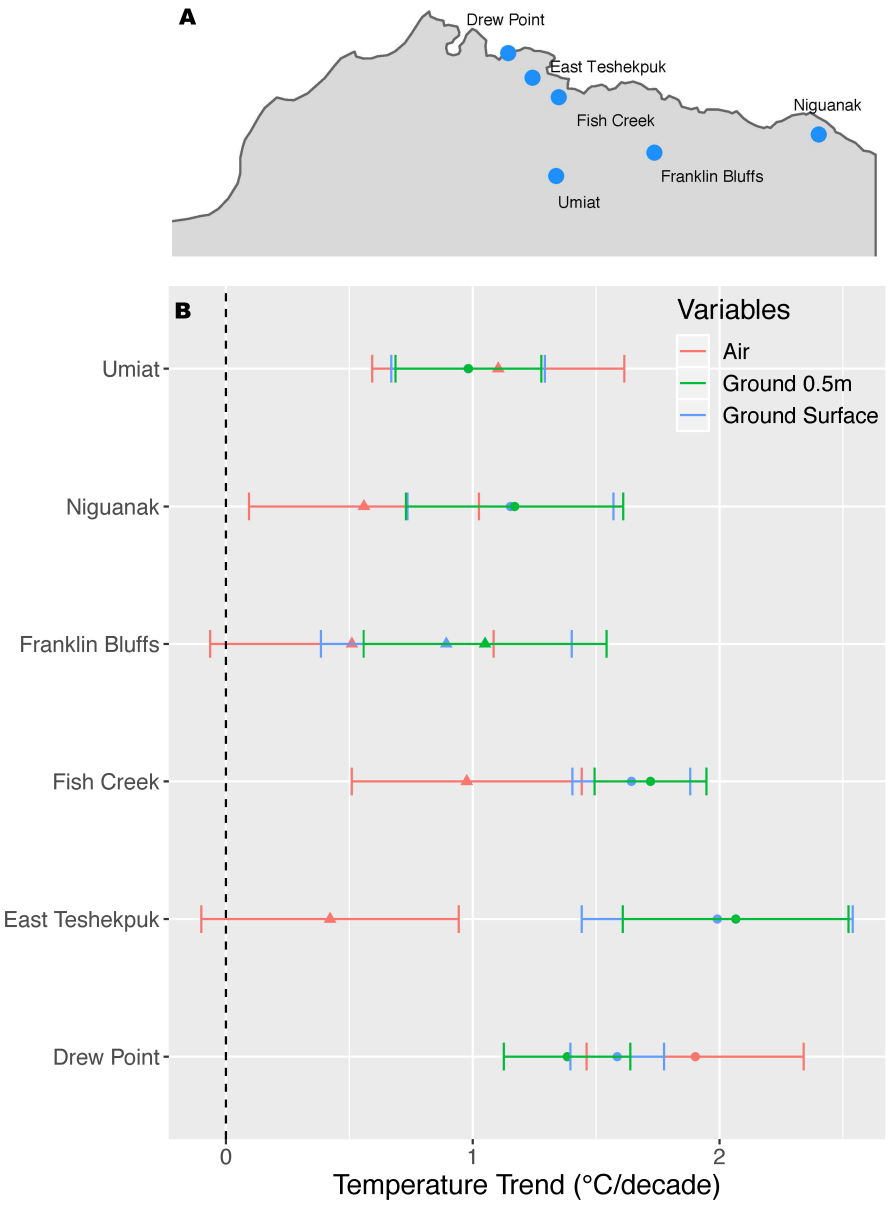

Figure 8. (A) Stations with at least ten years of identical period of air, ground surface and ground temperature at 0.5 m. (B) Trend comparison of air temperature, ground surface temperature, and ground temperature at 0.5 m over 1997-2016.Trends were estimated only for those stations comprising at least ten years of data. Error bars represent standard errors from the linear regression analysis. Circles indicate trends with p value ≤ 0.05, triangles indicate trends with p value >0.05.

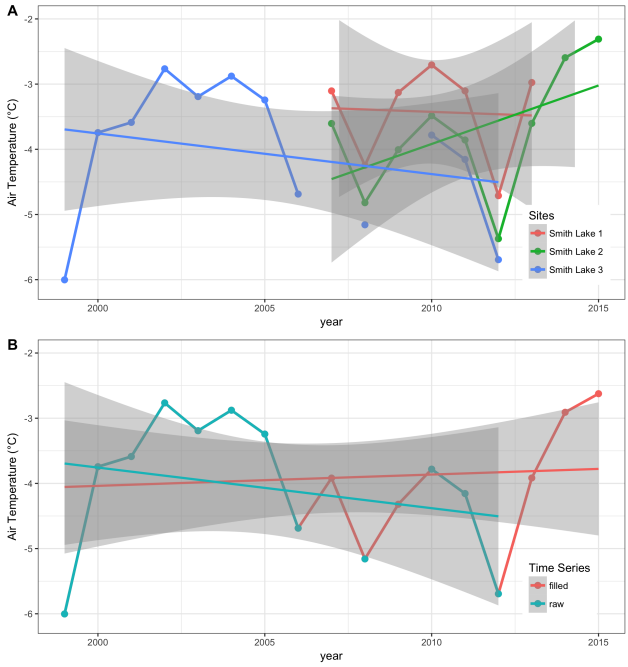

Figure 9. Comparison between A) trends calculated using measured data at SL1, SL2,and SL3; B) merged data series and corrected trends at SL3. The shadow shows standard error of the linear regression estimates.

Finally, we examined the physical relations among air temperature, snow cover and ground thermal state. Across these stations, effective snow depth was generally less than 0.4 m. The normalized temperature amplitude difference (ΔAmp_{norm}) that calculates the temperature difference between air and ground surface shows a positive linear relationship with effective snow depth. This correlation, so-called SHTM Slater et al. (2017), implies snow insulation effects increase with effective snow depth, which is consistent with previous studies (Burn and Smith, 1988; Demezhko and Shchapov, 2001; Zhang, 2005; Morse et al., 2012; Slater et al., 2017). In addition, while snow is considered an important factor on winter ground temperature, vegetation can also effect the amplitude through their influence on summer temperature.

4 Conclusions

Changes in near-surface ground temperatures over time are important indicators of a changing climate, because they provide vital information on the response of the ground to climate change. In this paper, we describe the data compilation process listing the work-flow and the challenges associated with preparing our synthesis permafrost dataset for Alaska. Standard unified protocols developed nationally and internationally to monitor near-surface permafrost conditions could significantly improve and simplify the development of corresponding permafrost benchmarks, and reduce the amount of time and effort required for data processing. This dataset consists of 41,667 monthly values during the data collection period (1997-2016). These data were

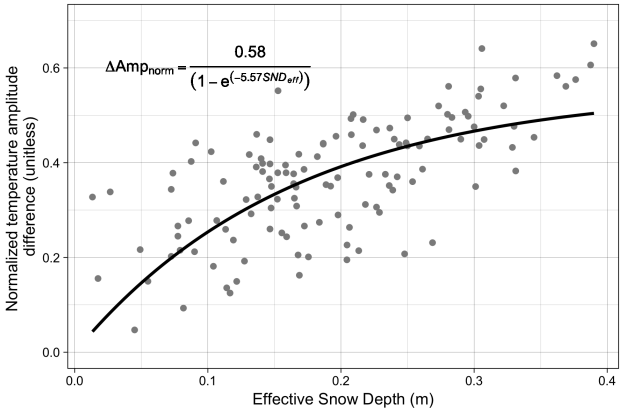

Figure 10. Correlation between effective snow depth and normalized temperature amplitude difference between air and ground surface. The mathematical function of fit line was following the correlation showed in Slater et al. (2017).

quality-controlled in data collection and data processing stages. We also implemented data harmonization validation for this compiled dataset. The PF-AK v0.1 can be easily integrated into model-data intercomparison tools such as International Land Model Benchmarking (ILAMB) tool (Luo et al., 2012). This dataset should be a valuable permafrost dataset and worth maintaining in the future. Widely, it also provides a prototype of basic data collection and management for remaining permafrost regions.

5 Data availability

The latest compiled dataset is available at the Arctic Data Center (https://doi.org/10.18739/A2KG55).

Competing interests. The authors declare that they have no conflict of interest.

Acknowledgements. We appreciate three Anonymous reviewers, Dr. David Swanson, and editor Dr.Chris DeBeer for their careful review and insightful comments which significantly strengthen our manuscript. We also appreciate all for producing and making their data available. This study was supported by the National Science Foundation (Award No. 1503559) and the NASA CMAC-14 project (No. NNX16AB19G). GC and FU were supported by the U.S. Geological Survey's Climate and Land Use Change Program. National Park Service data collection is supported by the NPS Inventory and Monitoring Program. GI-UAF Permafrost Lab data collection was supported by the National Science Foundation (Awards OPP-0120736, ARC-0632400, ARC-0520578, ARC-0612533, and ARC-1304271) and by the State of Alaska. TZ was supported by the National Natural Science Foundation of China (Award No. 91325202) and the National Key Scientific Research Program of China (Award No. 2013CBA01802). Any use of trade, firm, or product names is for descriptive purposes only and does not imply endorsement by the U.S. Government.

References

Abbott, B. W., Jones, J. B., Schuur, E. A. G., Chapin, F. S., Bowden, W. B., Bret-Harte, M. S., Epstein, H. E., Flannigan, M. D., Harms, T. K., Hollingsworth, T. N., Mack, M. C., McGuire, A. D., Natali, S. M., Rocha, A. V., Tank, S. E., Turetsky, M. R., Vonk, J. E., Wickland, K. P., Aiken, G. R., Alexander, H. D., Amon, R. M. W., Benscoter, B. W., Bergeron, Y., Bishop, K., Blarquez, O., Bond-Lamberty, B., Breen, A. L., Buffam, I., Cai, Y. H., Carcaillet, C., Carey, S. K., Chen, J. M., Chen, H. Y. H., Christensen, T. R., Cooper, L. W., Cornelissen, J. H. C., de Groot, W. J., DeLuca, T. H., Dorrepaal, E., Fetcher, N., Finlay, J. C., Forbes, B. C., French, N. H. F., Gauthier, S., Girardin, M. P., Goetz, S. J., Goldammer, J. G., Gough, L., Grogan, P., Guo, L. D., Higuera, P. E., Hinzman, L., Hu, F. S., Hugelius, G., Jafarov, E. E., Jandt, R., Johnstone, J. F., Karlsson, J., Kasischke, E. S., Kattner, G., Kelly, R., Keuper, F., Kling, G. W., Kortelainen, P., Kouki, J., Kuhry, P., Laudon, H., Laurion, I., Macdonald, R. W., Mann, P. J., Martikainen, P. J., McClelland, J. W., Molau, U., Oberbauer, S. F., Olefeldt, D., Pare, D., Parisien, M. A., Payette, S., Peng, C. H., Pokrovsky, O. S., Rastetter, E. B., Raymond, P. A., Raynolds, M. K., Rein, G., Reynolds, J. F., Robards, M., Rogers, B. M., Schadel, C., Schaefer, K., Schmidt, I. K., Shvidenko, A., Sky, J., Spencer, R. G. M., Starr, G., Striegl, R. G., Teisserenc, R., Tranvik, L. J., Virtanen, T., Welker, J. M., and Zimov, S.: Biomass offsets little or none of permafrost carbon release from soils, streams, and wildfire: an expert assessment, Environmental Research Letters, 11, 34 014–34 014, https://doi.org/10.1088/1748-9326/11/3/034014, 2016.

Bellingham, B. K.: Comprehensive Stevens Hydra Probe Users Manual, Report, 2015.

Bieniek, P. A., Walsh, J. E., Thoman, R. L., and Bhatt, U. S.: Using Climate Divisions to Analyze Variations and Trends in Alaska Temperature and Precipitation, Journal of Climate, 27, 2800–2818, https://doi.org/10.1175/Jcli-D-13-00342.1, 2014.

Biskaborn, B. K., Lanckman, J.-P., Lantuit, H., Elger, K., Streletskiy, D. A., Cable, W. L., and Romanovsky, V. E.: The new database of the Global Terrestrial Network for Permafrost (GTN-P), Earth System Science Data, 7, 245–259, https://doi.org/10.5194/essd-7-245-2015, https://www.earth-syst-sci-data.net/7/245/2015/, 2015.

Box, G., Hunter, J. S., and Hunter, W. G.: Statistics for experimenters: design, innovation, and discovery, vol. 2, Wiley-Interscience New York, 2005.

Brown, J., Ferrians, O., Heginbottom, J. A., and Melnikov., E.: Circum-Arctic Map of Permafrost and Ground-Ice Conditions, Version 2, http://nsidc.org/data/docs/fgdc/ggd318_map_circumarctic, 1998.

Brown, J., Hinkel, K. M., and Nelson, F. E.: The circumpolar active layer monitoring (calm) program: Research designs and initial results, Polar Geography, 24, 166–258, https://doi.org/10.1080/10889370009377698, 2000.

Burn, C. R. and Smith, C. A. S.: Observations of the Thermal Offset in near-Surface Mean Annual Ground Temperatures at Several Sites near Mayo, Yukon-Territory, Canada, Arctic, 41, 99–104, 1988.

Callaghan, T. V., Tweedie, C. E., Akerman, J., Andrews, C., Bergstedt, J., Butler, M. G., Christensen, T. R., Cooley, D., Dahlberg, U., Danby, R. K., Daniels, F. J., de Molenaar, J. G., Dick, J., Mortensen, C. E., Ebert-May, D., Emanuelsson, U., Eriksson, H., Hedenas, H., Henry, H. R. G., Hik, D. S., Hobbie, J. E., Jantze, E. J., Jaspers, C., Johansson, C., Johansson, M., Johnson, D. R., Johnstone, J. F., Jonasson, C., Kennedy, C., Kenney, A. J., Keuper, F., Koh, S., Krebs, C. J., Lantuit, H., Lara, M. J., Lin, D., Lougheed, V. L., Madsen, J., Matveyeva, N., McEwen, D. C., Myers-Smith, I. H., Narozhniy, Y. K., Olsson, H., Pohjola, V. A., Price, L. W., Riget, F., Rundqvist, S., Sandstrom, A., Tamstorf, M., Van Bogaert, R., Villarreal, S., Webber, P. J., and Zemtsov, V. A.: Multi-decadal changes in tundra environments and ecosystems: synthesis of the International Polar Year-Back to the Future project (IPY-BTF), Ambio, 40, 705–16, https://doi.org/10.1007/s13280-011-0179-8, 2011.

Clow, G. D.: Temperature data acquired from the DOI/GTN-P Deep Borehole Array on the Arctic Slope of Alaska, 1973â€“2013, Earth System Science Data, 6, 201–218, https://doi.org/10.5194/essd-6-201-2014, https://www.earth-syst-sci-data.net/6/201/2014/, 2014.

Demezhko, D. Y. and Shchapov, V. A.: 80,000 years ground surface temperature history inferred from the temperature–depth log measured in the superdeep hole SG-4 (the Urals, Russia), Global and Planetary Change, 29, 219–230, https://doi.org/https://doi.org/10.1016/S0921-8181(01)00091-1, 2001.

Hill, K. and Sousanes, P.: Climate station maintenance in the Central Alaska Inventory and Monitoring Network: 2015 summary, Report, 2015.

Hinzman, L. D., Deal, C. J., McGuire, A. D., Mernild, S. H., Polyakov, I. V., and Walsh, J. E.: Trajectory of the Arctic as an integrated system, Ecological Applications, 23, 1837–1868, https://doi.org/10.1890/11-1498.1, 2013.

IPCC: Climate change 2013: the physical science basis. Contribution of Working Group I to the Fifth Assessment Report of the Intergovernmental Panel on Climate Change [Stocker, T.F., D. Qin, G.-K. Plattner, M. Tignor, S.K. Allen, J. Boschung, A. Nauels, Y. Xia, Cambridge University Press, Cambridge, United Kingdom and New York, NY, USA, 2013.

Jorgenson, M., Yoshikawa, K., Kanevskiy, M., and Shur, Y.: Permafrost characteristics of Alaska, in: Proceedings of the Ninth International Conference on Permafrost, vol. 29, pp. 121–122, 2008.

Knoblauch, C., Beer, C., Liebner, S., Grigoriev, M. N., and Pfeiffer, E.-M.: Methane production as key to the greenhouse gas budget of thawing permafrost, Nature Climate Change, pp. 309–312, https://doi.org/10.1038/s41558-018-0095-z, 2018.

Koven, C. D., Lawrence, D. M., and Riley, W. J.: Permafrost carbon–climate feedback is sensitive to deep soil carbon decomposability but not deep soil nitrogen dynamics, Proceedings of the National Academy of Sciences, 112, 3752–3757, https://doi.org/10.1073/pnas.1415123112, 2015.

Liljedahl, A. K., Boike, J., Daanen, R. P., Fedorov, A. N., Frost, G. V., Grosse, G., Hinzman, L. D., Iijma, Y., Jorgenson, J. C., and Matveyeva, N.: Pan-Arctic ice-wedge degradation in warming permafrost and its influence on tundra hydrology, Nature Geoscience, 9, 312–318, https://doi.org/10.1038/ngeo2674, 2016.

Luo, Y. Q., Randerson, J. T., Abramowitz, G., Bacour, C., Blyth, E., Carvalhais, N., Ciais, P., Dalmonech, D., Fisher, J. B., Fisher, R., Friedlingstein, P., Hibbard, K., Hoffman, F., Huntzinger, D., Jones, C. D., Koven, C., Lawrence, D., Li, D. J., Mahecha, M., Niu, S. L., Norby, R., Piao, S. L., Qi, X., Peylin, P., Prentice, I. C., Riley, W., Reichstein, M., Schwalm, C., Wang, Y. P., Xia, J. Y., Zaehle, S., and Zhou, X. H.: A framework for benchmarking land models, Biogeosciences, 9, 3857–3874, https://doi.org/10.5194/bg-9-3857-2012, 2012.

McGuire, A. D., Koven, C., Lawrence, D. M., Clein, J. S., Xia, J., Beer, C., Burke, E., Chen, G., Chen, X., Delire, C., Jafarov, E., MacDougall, A. H., Marchenko, S., Nicolsky, D., Peng, S., Rinke, A., Saito, K., Zhang, W., Alkama, R., Bohn, T. J., Ciais, P., Decharme, B., Ekici, A., Gouttevin, I., Hajima, T., Hayes, D. J., Ji, D., Krinner, G., Lettenmaier, D. P., Luo, Y., Miller, P. A., Moore, J. C., Romanovsky, V., Schädel, C., Schaefer, K., Schuur, E. A. G., Smith, B., Sueyoshi, T., and Zhuang, Q.: Variability in the sensitivity among model simulations of permafrost and carbon dynamics in the permafrost region between 1960 and 2009, Global Biogeochemical Cycles, 30, 1015–1037, https://doi.org/10.1002/2016GB005405, 2016.

Melvin, A. M., Larsen, P., Boehlert, B., Neumann, J. E., Chinowsky, P., Espinet, X., Martinich, J., Baumann, M. S., Rennels, L., Bothner, A., Nicolsky, D. J., and Marchenko, S. S.: Climate change damages to Alaska public infrastructure and the economics of proactive adaptation, Proceedings of the National Academy of Sciences, 114, E122–E131, https://doi.org/10.1073/pnas.1611056113, 2017.

Menne, M. J., Williams, C. N., and Vose, R. S.: The U.S. Historical Climatology Network Monthly Temperature Data, Version 2, Bulletin of the American Meteorological Society, 90, 993–1007, https://doi.org/10.1175/2008bams2613.1, 2009.

Morse, P. D., Burn, C. R., and Kokelj, S. V.: Influence of snow on near-surface ground temperatures in upland and alluvial environments of the outer Mackenzie Delta, Northwest Territories, Canadian Journal of Earth Sciences, 49, 895–913, https://doi.org/10.1139/E2012-012, 2012.

Nelson, F. E. and Outcalt, S. I.: A computational method for prediction and regionalization of permafrost, Arctic and Alpine Research, pp. 279–288, 1987.

Plummer, N., Allsopp, T., Lopez, J. A., and Llansó, P.: Guidelines on Climate Observation: Networks and Systems, World Meteorological Organization, 2003.

Romanovsky, V., Marchenko, S., Daanen, R., Sergeev, D., and Walker, D.: Soil climate and frost heave along the permafrost/ecological North American Arctic transect, in: Proceedings of the Ninth International Conference on Permafrost, vol. 2, pp. 1519–1524, Institute of Northern Engineering: Fairbanks, AK, 2008.

Romanovsky, V., Cable, W., and Kholodov, A.: Changes in permafrost and active-layer temperatures along an Alaskan permafrost-ecological transect, in: Proc. 68th Canadian Geotechnical Conf. and Seventh Canadian Conf. on Permafrost (GEOQuébec 2015), 2015.

Schaefer, K., Lantuit, H., Romanovsky, V. E., Schuur, E. A. G., and Witt, R.: The impact of the permafrost carbon feedback on global climate, Environmental Research Letters, 9, 85 003–85 003, https://doi.org/10.1088/1748-9326/9/8/085003, 2014.

Sherstiukov, A.: Dataset of daily soil temperature up to 320 cm depth based on meteorological stations of Russian Federation, RIHMI-WDC, 176, 224–232, 2012.

Shiklomanov, N., Nelson, F., Streletskiy, D., Hinkel, K., and Brown, J.: The circumpolar active layer monitoring (CALM) program: data collection, management, and dissemination strategies, in: Proceedings of the ninth international conference on permafrost, vol. 29, Institute of Northern Engineering Fairbanks, Alaska, 2008.

Shiklomanov, N. I., Streletskiy, D. A., Swales, T. B., and Kokorev, V. A.: Climate Change and Stability of Urban Infrastructure in Russian Permafrost Regions: Prognostic Assessment Based on Gcm Climate Projections, Geographical Review, 107, 125–142, https://doi.org/10.1111/gere.12214, 2017.

Slater, A. G., Lawrence, D. M., and Koven, C. D.: Process-level model evaluation: a snow and heat transfer metric, Cryosphere, 11, 989–996, https://doi.org/10.5194/tc-11-989-2017, 2017.

Urban, F. E. and Clow, G. D.: DOI/GTN-P Climate and active-layer data acquired in the National Petroleum Reserve–Alaska and the Arctic National Wildlife Refuge, 1998–2015, Report 1021, https://doi.org/10.3133/ds1021, 2017.

Wang, K., Zhang, T., and Zhong, X.: Changes in the timing and duration of the near surface soil freeze/thaw status from 1956 to 2006 across China, Cryosphere, 9, 1321–1331, https://doi.org/10.5194/tc-9-1321-2015, 2015.

Wang, K., Zhang, T. J., Zhang, X. D., Clow, G. D., Jafarov, E. E., Overeem, I., Romanovsky, V., Peng, X. Q., and Cao, B.: Continuously amplified warming in the Alaskan Arctic: Implications for estimating global warming hiatus, Geophysical Research Letters, 44, 9029–9038, https://doi.org/10.1002/2017gl074232, 2017.

Yershov, E. D. and Williams, P. J.: General geocryology, Cambridge university press, 2004.

Zhang, T., Osterkamp, T. E., and Stamnes, K.: Influence of the Depth Hoar Layer of the Seasonal Snow Cover on the Ground Thermal Regime, Water Resources Research, 32, 2075–2086, https://doi.org/10.1029/96WR00996, 1996.

Zhang, T., Barry, R. G., Knowles, K., Heginbottom, J. A., and Brown, J.: Statistics and characteristics of permafrost and ground-ice distribution in the Northern Hemisphere, Polar Geography, 23, 132–154, https://doi.org/10.1080/10889379909377670, 1999.

Zhang, T. J.: Influence of the seasonal snow cover on the ground thermal regime: An overview, Reviews of Geophysics, 43, https://doi.org/10.1029/2004rg000157, 2005.

Table 1. Overview of the data from the permafrost monitoring stations in Alaska

					Number of available annual statistics							
Name	Latitude	Longitude	Onset	Last	MAAT	MAGST	MAGT 0.25 m	MAGT 0.5 m	MAGT 0.75 m	MAGT 1 m	Snow Depth	Source
Awuna1	69.17	-158.01	1998	2004	3	2	2	2	2	2	1	USGS
Awuna2	69.16	-158.03	2003	2015	7	1	1	1	1	1	5	USGS
Camden Bay	69.97	-144.77	2003	2015	7		1	1	1	1	1	USGS
Drew Point	70.86	-153.91	1998	2015	11	12	12	12	12	12	8	USGS
East Teshekpuk	70.57	-152.97	2004	2015	1	1	1	1	1	1	1	USGS
Fish Creek	70.34	-152.05	1998	2015	14	15	15	15	15	15	11	USGS
Ikpikpuk	70.44	-154.37	2005	2015	9	4	5				5	USGS
Inigok	69.99	-153.09	1998	2015	12	7	1	1	1	1	14	USGS
Koluktak	69.75	-154.62	1999	2015	9	6	11	11	11	11	1	USGS
Lake145Shore	70.69	-152.63	2007	2015	4						5	USGS
Marsh Creek	69.78	-144.79	2001	2015	12	1	7	7	7	7	12	USGS
Niguanak	69.89	-142.98	2000	2015	14	14	14	14	14	14	11	USGS
Piksiksak	70.04	-157.08	2004	2015	1	7	1	1	1	1	8	USGS
Red Sheep Creek	68.68	-144.84	2004	2015	7	1	6	6	6	6	7	USGS
South Meade	70.63	-156.84	2003	2015	1	8	1	1	1	1	8	USGS
Tunalik	70.20	-161.08	1998	2015	13	8	14	14	14	14	13	USGS
Umiat	69.40	-152.14	1998	2015	14	13	13	13	13	13	11	USGS
Barrow 2	71.31	-156.66	2002	2016	4	9	8	8	8	6	4	GI-UAF
Boza Creek 1	64.71	-148.29	2009	2016	6	1	6	6	6	6	5	GI-UAF
Boza Creek 2	64.72	-148.29	2009	2016	6	6	6	6	6	6		GI-UAF
Chandalar Shelf	68.07	-149.58	1997	2016	11	11	14	14	2			GI-UAF
Deadhorse	70.16	-148.47	1997	2016	3	3	4	4	4			GI-UAF
Fox	64.95	-147.62	2001	2016	3		5	5	4			GI-UAF
Franklin Bluffs	69.67	-148.72	1997	2016	13	1	13	13	8			GI-UAF
Franklin Bluffs boil	69.67	-148.72	2007	2016		4	8	8	8			GI-UAF
Franklin Bluffs interior boil	69.67	-148.72	2006	2016		6	9	7	6			GI-UAF
Franklin Bluffs Wet	69.68	-148.72	2006	2016	3	3	3	3	5			GI-UAF
Galbraith Lake	68.48	-149.50	2001	2016	6	6	6	6	6			GI-UAF
Happy Valley	69.16	-148.84	2001	2016	6	8	8	8	8		4	GI-UAF
Imnaviat	68.64	-149.35	2006	2016	8	8	8	8	8			GI-UAF
Ivotuk 3	68.48	-155.74	2006	2013	2	2	2	2	2			GI-UAF
Ivotuk 4	68.48	-155.74	1998	2016	6	5	5	5	4	1	6	GI-UAF
Pilgrim Hot Springs	65.09	-164.90	2012	2016	2	2	2	2	2	2	3	GI-UAF
Sag1 MNT (Moist Non-Acidic Tundra)	69.43	-148.67	2001	2016	7	3	12	12	12	1		GI-UAF
Sag2 MAT (Moist Acidic Tundra)	69.43	-148.70	2001	2016		11	11	11	11	3		GI-UAF
Selawik Village	66.61	-160.02	2012	2016	3	3	3	3	3	3	3	GI-UAF

Table 1. Overview of the data from the permafrost monitoring stations in Alaska—continued.

					Number of available annual statistics							
Name	Latitude	Longitude	Onset	Last	MAAT	MAGST	MAGT 0.25 m	MAGT 0.5 m	MAGT 0.75 m	MAGT 1 m	Snow Depth	Source
Smith Lake 1	64.87	-147.86	1997	2016	9	9	9	9	9	9		GI-UAF
Smith Lake 2	64.87	-147.86	2006	2016	9	7	9	9	9	9		GI-UAF
Smith Lake 3	64.87	-147.86	1997	2016	12	5	5	8	8	8		GI-UAF
Smith Lake 4	64.87	-147.86	2006	2016	7	7	4	4	4	7		GI-UAF
UAF Farm	64.85	-147.86	2007	2016	7	6	7	7	5	5	4	GI-UAF
West Dock	70.37	-148.55	2001	2016	9	4	11	11	11		3	GI-UAF
Gakona 1	62.39	-145.15	2009	2016	5	5	5	5	5	5		GI-UAF
Gakona 2	62.39	-145.15	2009	2016	5	5	5	5	5	3		GI-UAF
ASIA2	67.47	-162.27	2012	2016	3		3	3			2	NPS
CCLA2	65.31	-143.13	2004	2016	11		9	11	11		8	NPS
CHMA2	67.71	-150.59	2012	2016	3		3	3	2		2	NPS
CREA2	62.12	-141.85	2004	2016	11	5	1	1	5	5	11	NPS
CTUA2	61.27	-142.62	2004	2016	11	5	11	11			9	NPS
DKLA2	63.27	-149.54	2004	2016	9		4	4	4	4	7	NPS
DVLA2	66.28	-164.53	2011	2016	4		3	3				NPS
ELLA2	65.28	-163.82	2012	2016	3		3	3			1	NPS
GGLA2	61.60	-143.01	2005	2016	1	5	9	1			5	NPS
HOWA2	68.16	-156.90	2011	2016	3		2	2			1	NPS
IMYA2	67.54	-157.08	2012	2016	3		3	3			1	NPS
KAUA2	67.57	-158.43	2012	2016	3		3	3			1	NPS
KLIA2	67.98	-155.01	2012	2016	2		2	2			1	NPS
KUGA2	68.32	-161.49	2014	2016	1		1	1			1	NPS
MITA2	65.82	-164.54	2011	2016								NPS
MNOA2	67.14	-162.99	2011	2016	4		2	2	2		1	NPS
PAMA2	67.77	-152.16	2012	2016	2		2	2			2	NPS
RAMA2	67.62	-154.34	2012	2016	1		1	1				NPS
RUGA2	62.71	-150.54	2008	2016	4						2	NPS
SRTA2	65.85	-164.71	2011	2016	4		2	2			3	NPS
SRWA2	67.46	-159.84	2011	2016	1		1	1			2	NPS
SSIA2	68.00	-160.40	2011	2016	4		3	3	2		2	NPS
TAHA2	67.55	-163.57	2011	2016	3		1	1	1		3	NPS
TANA2	60.91	-142.90	2005	2016	5		2	2			3	NPS
TEBA2	61.18	-144.34	2005	2016	8		5	5			6	NPS
TKLA2	63.52	-150.04	2005	2016	1	1					8	NPS
UPRA2	64.52	-143.20	2005	2016	9	3	6	6			4	NPS
WIGA2	63.81	-150.11	2013	2016	2		2	2			1	NPS

Table 2. Brief description of vegetation and soil type of monitoring stations in Alaska

Name	Vegetation	Soil Type	Name	Vegetation	Soil Type
Drew Point	Moist-meadow, tussock-tundra complex	Silt	Selawik Village	Upland DwarfBirch-Tussock Shrub	-
Fish Creek	Moist-meadow, tussock-tundra complex	Silt	Smith Lake 1	White Spruce forest with high canopy	-
Inigok	Moist-meadow, tussock-tundra complex	Silt	Smith Lake 2	Dense diminutive Black Spruce forest	-
Tunalik	Moist-meadow, tussock-tundra complex	Silty Sand	Smith Lake 3	Forest surrounded by Black Spruce trees and	-
Umiat	Moist-tussock tundra	Silt		tussock-shrubs	
Barrow 2	Graminoid-moss tundra (wet and moist acidic)	Typic Histoturbel, Typic Aquiturbel	Smith Lake 4	Hummocks of sedges (tussocks) and shrubby vegetation with sparse Black Spruce	-
Boza Creek 1	Open black spruce forest	Pergelic Cryaquepts	West Dock	Moist to wet tundra	Typic Aquahaplel
Boza Creek 2		-	ASIA2	Dryas octapetala	Lithic Haplogelept
Chandalar Shelf	Alpine meadow with low shrubs	Ruptic-Histic Aquiturbel	DVLA2	Arctagrostic latifolia, Petasites frigidus, Carex	Aquic Molliturbel
Deadhorse	Graminoid-moss tundra and graminoid, prostrate-dwarf-shrub, moss tundra (wet and moist nonacidic)	Terric Aquiturbel		bigelowii, Empetrum hermaphroditum, Ledum palustre, Vaccinium uliginosum, Arctous alpina, Hylocomium splendens, Lupinus arcticus, Salix pulchra	
Franklin Bluffs	Graminoid-moss tundra and graminoid, prostrate-dwarf-shrub, moss tundra	Ruptic-Histic Aquorthel	ELLA2	Umbilicaria, Alectoria migricans, Carex	Typic Haploturbel
Franklin Bluffs Wet	Graminoid-moss tundra and graminoid, prostrate-dwarf-shrub, moss tundra	-	HOWA2	Dryas octopetala, Salix phlebophylla	Typic Gelorthent
			IMYA2	Dryas octopetala, Hierchloe alpine, Salix phlebophylla	Typic Gelorthent
Galbraith Lake	Graminoid-moss tundra and graminoid, prostrate-dwarf-shrub, moss tundra (wet and moist nonacidic)	Ruptic-Histic Aquiturbel	KAUA2	Dryas octopetala, Vaccinium uliginosum	Typic Gelorthent
			KUGA2	Betula, Empetrum hermaphroditum, Ledium palustre, Vaccinium vitis-ideae	Typic Gelorthent
Happy Valley	Tussock-graminoid, dwarf- shrub tundra and low-shrub tundra (moist acidic)	Ruptic-Histic Aquiturbel	MNOA2	Dryas integrifolia, Potentilla biflora	Typic Haploturbel
Imnaviat	Tussock-graminoid, dwarf- shrub tundra and low-shrub tundra (moist acidic)	Typic Histoturbel, Typic Aquorthel	SRTA2	Betula, Ledum palustre, Loiseleuria procumbens, Stereocaulon, Flavocetraria cucullata, Vaccinium uliginosum	Typic Haplogelept
Ivotuk 3	Horsetail-rich variation of nonacidic tundra	-			
Ivotuk 4	Moss dominated	-	SRWA2	Betula, Dryas octopetala	Typic Gelorthent
Sag1 MNT (Moist Non-Acidic Tundra)	Moist nonacidic tundra	Pergelic Cryaquolls (43%), P. Cryaquepts (18%), P. Cryoborolls (14%), others (25%)	SSIA2	Dryas octapetala, Arctous alpinus, Lupinus arcticus, Rhytidium rugosum	Typic Haplorthel
			TAHA2	Betula, Dryas octapetala, Vaccinium uliginosum, Salix phlebophylla	Typic Gelorthent
Sag2 MAT (Moist Acidic Tundra)	Moist acidic tundra	Pergelic Cryaquepts (79%), Histic Pergelic Cryaquepts (21%)	UPRA2	Betula, Empetrum hermaphroditum, Ledum palustre, Picea glauca	Typic Dystrogelept

Table 3. Summary of ground temperature instruments from USGS, GI-UAF, and NPS networks of Alaska, USA.

Network	Temperature sensor	Datalogger	Measurement Depths ($^{\circ}C$)	Temperature Ranges ($^{\circ}C$)	Accuracy	Maintenance visits
USGS	MRC thermistor	CR10X or CR1000	Surface, 0.10, 0.20, 0.25, 0.30, 0.45, 0.70, 0.95, and 1.20 m (except for Lake145Shore, where was only 0.25 m available)	-30 to 75	0.01	July, August
GI-UAF	Campbell Scientific 107	CR10x or CR1000	Surface to >1 m, but various in stations	-35 to 50	0.02	July, August
	MRC thermistor	CR10x or CR1000	Surface to >1 m, but various in stations	-30 to 75	0.01	July, August
NPS	Campbell Scientific 107	CR-1000 XT	Surface, 0.10, 0.20, 0.50, 0.75, and 1.00 m, but various in stations	-35 to 50	0.02	July, August

Table 4. Summary of the air, ground surface, ground temperature at 1 m, volumetric water content and snow depth over the entire observation period.

	Air Temperature ($^{\circ}C$)			Ground Surface Temperature ($^{\circ}C$)			Ground Temperature at 1 m ($^{\circ}C$)			VWC (m^3/m^3)			Snow Depth (m)	
Site	Min	Mean	Max	Min	Mean	Max	Min	Mean	Max	Min	Mean	Max	Mean	Max
Awuna1	-28.51	-10.61	9.62	-11.30	-4.16	2.79	-9.38	-4.52	-0.93				0.39	0.61
Awuna2	-30.47	-9.88	11.60	-13.21	-3.34	8.10	-10.84	-4.43	-0.64	0.02	0.21	0.43	0.37	0.54
Camden Bay	-28.89	-10.35	6.92				-14.47	-7.49	-1.20				0.20	0.26
Drew Point	-28.62	-10.84	6.04	-20.60	-7.63	4.74	-16.02	-7.84	-1.68				0.18	0.29
East Teshekpuk	-28.19	-10.27	7.79	-17.97	-6.26	4.07	-14.20	-6.91	-1.90	0.01	0.18	0.42	0.23	0.32
Fish Creek	-29.07	-10.55	8.81	-16.85	-6.02	4.50	-14.11	-6.82	-1.17	0.01	0.17	0.41	0.20	0.28
Ikpikpuk	-29.15	-10.27	9.21	-18.08	-5.49	5.60							0.22	0.37
Inigok	-29.98	-10.58	10.55	-16.28	-4.80	7.73	-12.68	-5.58	-0.60	0.00	0.12	0.33	0.22	0.33
Koluktak	-30.02	-10.18	11.64	-15.20	-3.77	8.75	-13.77	-4.69	1.16	0.02	0.13	0.36	0.20	0.30
Lake145Shore	-28.72	-10.50	7.30							0.06	0.21	0.41	0.28	0.42
Marsh Creek	-26.51	-8.65	10.20	-16.87	-5.28	5.26	-14.39	-6.11	-0.82	0.03	0.16	0.41	0.19	0.25
Niguanak	-27.80	-9.97	8.48	-18.13	-6.09	4.66	-14.87	-6.72	-1.02				0.15	0.21
Piksiksak	-29.21	-9.93	10.71	-17.65	-5.76	6.21	-13.44	-5.94	-0.87				0.10	0.16
Red Sheep Creek	-23.94	-6.81	12.88	-10.04	-2.76	8.84	-8.78	-3.56	-0.36	0.02	0.25	0.74	0.23	0.38
South Meade	-29.90	-10.42	9.35	-19.91	-6.45	5.89	-15.74	-7.19	-1.12				0.19	0.29
Tunalik	-28.26	-10.17	9.15	-21.58	-7.12	6.81	-16.18	-7.35	-0.92				0.17	0.28
Umiat	-28.67	-9.84	11.18	-14.24	-4.66	4.71	-10.96	-5.14	-1.04				0.32	0.44
Barrow 2	-26.55	-10.23	5.09	-19.17	-6.87	5.33	-15.46	-7.41	-1.59	0.02	0.16	0.39	0.14	0.22
Boza Creek 1	-25.00	-3.20	16.03	-9.17	1.13	12.93	-4.58	-1.27	-0.29	0.00	0.20	0.55	0.18	0.36
Boza Creek 2	-23.60	-2.18	16.31	-3.62	2.28	12.00	-0.46	0.09	1.23	0.06	0.22	0.40		
Chandalar Shelf	-23.66	-7.64	11.41	-9.54	-1.29	7.74				0.00	0.22	0.74		
Deadhorse	-28.04	-9.97	8.27	-14.89	-3.65	7.13				0.03	0.16	0.38		
Fox	-26.02	-2.99	16.03							0.08	0.24	0.40		
Franklin Bluffs	-30.15	-10.62	10.74	-14.65	-3.89	8.38				0.02	0.19	0.47		
Franklin Bluffs boil				-18.04	-4.15	11.99								
Franklin Bluffs interior boil				-16.85	-3.66	11.12								
Franklin Bluffs Wet	-28.56	-10.49	10.84	-14.52	-3.36	10.28								
Galbraith Lake	-28.77	-9.35	10.72	-14.38	-3.45	9.34								
Happy Valley	-30.01	-9.49	12.30	-9.31	-1.63	7.19				0.02	0.14	0.31	0.27	0.47
Imnaviat	-22.95	-6.81	10.57	-8.48	-0.81	8.54								
Ivotuk 3	-29.85	-10.12	11.30	-9.97	-1.14	6.99								
Ivotuk 4	-29.10	-9.70	11.23	-9.21	-1.24	8.26	-5.16	-1.89	-0.53	0.00	0.27	0.77	0.43	0.60
Pilgrim Hot Springs	-16.78	-2.04	14.63	-11.95	0.08	13.52	-7.56	-2.30	-0.27	0.00	0.30	0.73	0.06	0.21
Sag1 MNT	-26.72	-8.39	10.68	-17.14	-4.27	9.48	-13.50	-5.00	0.24	0.04	0.20	0.40		
Sag2 MAT				-15.11	-3.76	9.01	-11.03	-4.49	-0.45	0.02	0.26	0.63		
Selawik Village	-20.26	-3.72	14.91	-11.16	-0.74	12.18	-7.99	-3.09	-0.45				0.05	0.12

Table 4. Summary of the air, ground surface, ground temperature at 1 m, volumetric water content and snow depth over the entire observation period—continued.

	Air Temperature ($^{\circ}C$)			Ground Surface Temperature ($^{\circ}C$)			Ground Temperature at 1 m ($^{\circ}C$)			VWC (m^3/m^3)			Snow Depth (m)	
Site	Min	Mean	Max	Min	Mean	Max	Min	Mean	Max	Min	Mean	Max	Mean	Max
Smith Lake 1	-23.88	-3.06	16.06	-11.29	-0.11	12.98	-2.02	-0.73	-0.26	0.02	0.14	0.31		
Smith Lake 2	-24.91	-3.74	15.98	-7.32	1.10	12.86	-4.10	-1.11	0.00	0.07	0.29	0.59		
Smith Lake 3	-27.29	-4.70	14.68	-3.49	2.57	11.51	-0.33	0.00	0.88	0.07	0.23	0.40		
Smith Lake 4	-26.15	-3.58	18.20	-15.81	-2.27	9.68	-10.32	-3.81	-0.62					
UAF Farm	-22.09	-1.48	16.57	-10.91	0.68	13.00	-0.83	1.18	5.43				0.28	0.47
West Dock	-28.82	-10.53	6.81	-20.30	-6.68	5.46				0.01	0.20	0.55	0.04	0.09
Gakona 1	-23.06	-2.76	13.70	-5.29	1.55	11.26	-1.62	-0.63	-0.22					
Gakona 2	-23.01	-2.45	14.00	-5.54	1.35	9.63	-0.72	-0.18	0.75					
ASIA2	-15.10	-3.20	12.24										0.02	0.07
CCLA2	-27.39	-4.52	15.90										0.33	0.52
CHMA2	-15.97	-5.24	9.81										0.04	0.08
CREA2	-16.41	-3.87	8.57	-12.35	-1.78	11.22	-6.00	-2.13	0.35				0.12	0.21
CTUA2	-14.15	-2.52	8.61	-12.83	-1.09	12.43							0.08	0.16
DKLA2	-17.19	-3.32	10.72				-3.33	1.22	7.03				0.39	0.64
DVLA2	-21.84	-5.38	10.77											
ELLA2	-17.18	-4.81	9.93										0.29	0.43
GGLA2	-13.51	-2.01	9.13	-1.50	2.54	12.18							0.90	1.45
HOWA2	-23.29	-6.64	10.18										0.05	0.11
IMYA2	-15.30	-5.19	8.96										0.15	0.26
KAUA2	-21.65	-6.47	10.01										0.15	0.25
KLIA2	-19.10	-7.66	7.38										0.07	0.10
KUGA2	-16.74	-3.56	13.64										0.18	0.59
MITA2														
MNOA2	-18.78	-3.79	12.47										0.14	0.37
PAMA2	-18.00	-4.49	11.02										0.07	0.11
RAMA2	-17.93	-5.42	10.77											
RUGA2	-9.49	-0.53	10.45										0.50	0.83
SRTA2	-21.96	-4.69	11.77										0.06	0.16
SRWA2	-17.35	-3.15	13.89										0.34	0.68
SSIA2	-21.85	-5.86	11.27										0.02	0.06
TAHA2	-20.09	-4.48	11.58										0.09	0.20
TANA2	-13.83	-2.02	9.91										1.01	1.55
TEBA2	-17.27	-1.92	11.54										0.75	1.34
TKLA2	-18.48	-3.15	11.39	-6.93	1.63	13.17							0.15	0.25
UPRA2	-21.39	-4.91	11.36	-13.19	-1.69	12.80							0.33	0.48
WIGA2	-17.84	-1.55	13.21										0.10	0.15

Table 5. Summary of freezing (DDF, $^{\circ}C - day$), thawing index (DDT, $^{\circ}C - day$) and Frost Number (FN, unitless) of air and ground temperatures over the entire observation period.

	Air			Ground Surface			Ground 0.25 m			Ground 0.50 m			Ground 0.75 m			Ground 1.00 m		
Site	DDF	DDT	FN	DDF	DDT	FN	DDF	DDT	FN	DDF	DDT	FN	DDF	DDT	FN	DDF	DDT	FN
Awuna1	4217	769	0.70	1750	196	0.75	1862	10	0.93	1878	0	1.00	1880	0	1.00	1880	0	1.00
Awuna2	4417	975	0.68	1740	807	0.59	1939	233	0.74	2086	7	0.95	2121	0	1.00	2095	0	1.00
Camden Bay	4493	482	0.75				2684	100	0.84	2858	0	1.00	2873	0	1.00	2860	0	1.00
Drew Point	4521	400	0.77	3221	327	0.76	3291	46	0.89	3280	0	1.00	3248	0	1.00	3231	0	1.00
East Teshekpuk	4298	576	0.73	2815	279	0.76	2964	18	0.93	2982	0	1.00	2951	0	1.00	2939	0	1.00
Fish Creek	4376	677	0.72	2582	328	0.74	2813	12	0.94	2821	0	1.00	2804	0	1.00	2789	0	1.00
Ikpikpuk	4356	718	0.71	2712	434	0.71	2685	225	0.78									
Inigok	4404	858	0.69	2268	708	0.64	2454	60	0.86	2491	0	1.00	2449	0	1.00	2423	0	1.00
Koluktak	4337	984	0.68	2034	856	0.61	2242	618	0.66	2309	325	0.73	2340	153	0.80	2355	54	0.87
Lake145Shore	4430	522	0.74															
Marsh Creek	3836	860	0.68	2526	408	0.71	2831	159	0.81	2863	20	0.92	2801	0	1.00	2776	0	1.00
Niguanak	4179	654	0.72	2798	339	0.74	2952	54	0.88	2960	1	0.98	2934	0	1.00	2900	0	1.00
Piksiksak	4263	886	0.69	2594	506	0.69	2700	66	0.86	2707	0	1.00	2657	0	1.00	2611	0	1.00
Red Sheep Creek	3249	1230	0.62	1208	989	0.52	1637	324	0.69	1715	58	0.84	1710	0	1.00	1667	0	1.00
South Meade	4477	727	0.71	3006	447	0.72	3186	45	0.89	3214	0	1.00	3187	0	1.00	3078	0	1.00
Tunalik	4213	725	0.71	3230	535	0.71	3258	138	0.83	3225	8	0.95	3160	0	1.00	3120	0	1.00
Umiat	4138	948	0.68	2114	374	0.70	2306	14	0.93	2271	0	1.00	2216	0	1.00	2189	0	1.00
Barrow 2	4241	325	0.78	2925	398	0.73	2996	85	0.86	3072	0	1.00	3049	0	1.00	3112	0	1.00
Boza Creek 1	3270	1634	0.59	959	1646	0.43	676	581	0.52	832	81	0.76	917	1	0.97	888	0	1.00
Boza Creek 2	3036	1704	0.57	278	1808	0.28	224	839	0.34	166	550	0.35	103	308	0.37			
Chandalar Shelf	3285	1049	0.64	1184	855	0.54	1352	55	0.83	1302	0	1.00	1388	0	1.00			
Deadhorse	4236	628	0.72	2070	654	0.64	2106	261	0.74	2144	101	0.82	2236	3	0.96			
Fox	3441	1618	0.59				192	442	0.40	214	21	0.76	191	0	1.00			
Franklin Bluffs	4420	879	0.69	1964	820	0.61	2096	237	0.75	2114	61	0.85	2289	1	0.98			
Franklin Bluffs boil				2339	1234	0.58	2293	792	0.63	2117	414	0.69	2018	193	0.76			
Franklin Bluffs interior boil				2192	1145	0.58	2132	498	0.67	2166	288	0.73	2073	111	0.81			
Franklin Bluffs Wet	4142	907	0.68	1873	1100	0.57	1733	635	0.62	1734	689	0.61	1702	68	0.83			
Galbraith Lake	4190	895	0.68	1875	955	0.58	2050	167	0.78	2110	14	0.92	2123	0	1.00			
Happy Valley	4293	1061	0.67	1167	781	0.55	1245	211	0.71	1337	36	0.86	1404	0	1.00			
Imnaviat	3212	954	0.65	994	1005	0.50	1017	460	0.60	1053	218	0.69	1086	93	0.77			
Ivotuk 3	4332	948	0.68	1273	729	0.57	1134	127	0.75	1312	3	0.95	1312	0	1.00			
Ivotuk 4	4209	948	0.68	1105	933	0.52	1142	579	0.58	1248	120	0.76	1290	6	0.94	1038	0	1.00
Pilgrim Hot Springs	2025	1632	0.53	1346	1631	0.48	1723	168	0.76	1583	18	0.90	1465	1	0.97	1427	0	1.00
Sag1 MNT (Moist Non-Acidic Tundra)	3840	912	0.67	2313	914	0.61	2209	521	0.67	2227	202	0.77	2259	36	0.89	2425	5	0.96
Sag2 MAT (Moist Acidic Tundra)				2012	900	0.60	2207	186	0.78	2287	44	0.88	2281	12	0.93	2098	3	0.96

Table 5. Summary of freezing (DDF, $^{\circ}C - day$), thawing index (DDT, $^{\circ}C - day$) and Frost Number (FN, unitless) of air and ground temperatures over the entire observation period—continued.

	Air			Ground Surface			Ground 0.25 m			Ground 0.50 m			Ground 0.75 m			Ground 1.00 m		
Site	DDF	DDT	FN	DDF	DDT	FN	DDF	DDT	FN	DDF	DDT	FN	DDF	DDT	FN	DDF	DDT	FN
Selawik Village	2556	1579	0.56	1266	1452	0.48	1626	148	0.77	1695	0	1.00	1608	0	1.00	1542	0	1.00
Smith Lake 1	3086	1659	0.58	1273	1581	0.47	488	70	0.73	469	1	0.96	429	0	1.00	415	0	1.00
Smith Lake 2	3254	1624	0.59	712	1723	0.39	779	392	0.59	810	120	0.72	781	13	0.89	748	1	0.96
Smith Lake 3	3510	1482	0.61	275	1739	0.28	227	773	0.35	114	514	0.32	60	324	0.30	36	137	0.34
Smith Lake 4	3384	1934	0.57	2084	966	0.59	1815	353	0.69	2064	39	0.88	2082	0	1.00	1996	0	1.00
UAF Farm	2779	1773	0.56	1216	1599	0.47	499	1043	0.41	279	959	0.35	135	949	0.27	51	891	0.19
West Dock	4491	475	0.75	3108	400	0.74	3181	22	0.92	3186	0	1.00	3121	0	1.00			
Gakona 1	3068	1361	0.60	483	1573	0.36	434	303	0.54	443	35	0.78	437	0	1.00	336	0	1.00
Gakona 2	3046	1402	0.60	564	1311	0.40	428	578	0.46	261	294	0.49	160	233	0.45	139	145	0.49
ASIA2	1861	1339	0.54				1657	1150	0.55	1617	1030	0.56						
CCLA2	3656	1559	0.60				1430	551	0.62	1162	23	0.88	1113	3	0.95			
CHMA2	2104	981	0.59				2222	936	0.61	1837	478	0.66	1537	358	0.67			
CREA2	2248	817	0.62	1481	1274	0.52	1412	725	0.58	1267	396	0.64	1131	129	0.75	1046	15	0.89
CTUA2	1880	868	0.60	1510	1438	0.51	1434	870	0.56	1310	751	0.57						
DKLA2	2264	1084	0.59				725	1350	0.42	566	1216	0.41	428	1098	0.38	321	997	0.36
DVLA2	3031	1010	0.63				1742	360	0.69	1724	143	0.78						
ELLA2	2298	975	0.61				1545	1030	0.55	1530	760	0.59						
GGLA2	1753	953	0.58	79	2028	0.16	17	1824	0.09	4	1642	0.05						
HOWA2	3292	901	0.66				3295	678	0.69	3111	516	0.71						
IMYA2	2038	880	0.60				1849	995	0.58	1887	547	0.65						
KAUA2	3027	904	0.65				1764	623	0.63	1674	452	0.66						
KLIA2	2763	624	0.68				2201	366	0.71	2257	208	0.77						
KUGA2	2057	1491	0.54				1255	1418	0.48	1245	1066	0.52						
MITA2																		
MNOA2	2447	1295	0.58				963	1050	0.49	1144	959	0.52	1059	704	0.55			
PAMA2	2374	1101	0.59				2135	611	0.65	2117	409	0.69						
RAMA2	2373	1066	0.60				1916	952	0.59	1854	1036	0.57						
RUGA2	1075	1250	0.48															
SRTA2	2998	1138	0.62				1192	1147	0.50	1063	1122	0.49						
SRWA2	2142	1510	0.54				928	1826	0.42	786	1516	0.42						
SSIA2	2993	1062	0.63				2234	771	0.63	2165	608	0.65	1789	526	0.65			
TAHA2	2702	1149	0.61				1590	1175	0.54	1565	1027	0.55	1399	631	0.60			
TANA2	1770	1053	0.56				171	1850	0.23	106	1505	0.21						
TEBA2	2237	1191	0.58				66	1985	0.15	28	1757	0.11						
TKLA2	2446	1151	0.59	669	1809	0.38												
UPRA2	2913	1083	0.62	1552	1481	0.51	1084	1142	0.49	884	832	0.51						
WIGA2	2246	1402	0.56				1053	289	0.66	1120	59	0.81						